

Review

Metal ion catalysis in acyl and phosphoryl transfer: Transition states as ligands

Anatoly K. Yatsimirsky*

Facultad de Química, Universidad Nacional Autónoma de México, 04510 México D.F., Mexico

Received 8 September 2004; accepted 15 April 2005

Available online 6 June 2005

Contents

1. Introduction	1997
2. Calculation of the binding constant of the catalyst to the transition state of the uncatalyzed reaction	1998
3. Transition states for uncatalyzed hydrolyses of carboxylic acid and phosphate esters	2000
4. Transition state binding constants for catalytic hydrolyses	2002
4.1. Carboxylic acid esters	2002
4.2. Phosphate triesters	2006
4.3. Phosphate diesters	2007
5. Conclusions	2009
Acknowledgements	2010
References	2010

Abstract

Interpretation of the role of metal ions in catalysis in terms of direct binding of the catalyst to the transition state of the uncatalyzed reaction allows one to view transition states as ligands and to apply the concepts elaborated for analysis of stability of coordination compounds to reactivity. This paper reviews recent results on kinetics of metal ion catalyzed hydrolysis of carboxylic acid and phosphate esters providing pseudo-equilibrium transition state complexation constants (K_T^\ddagger) for approximately 130 reactions. General trends in K_T^\ddagger values, in particular, interrelations between ground state and transition state complexation for different groups of catalysts and reactions are discussed.

© 2005 Elsevier B.V. All rights reserved.

Keywords: Catalysis; Transition state; Hydrolysis

1. Introduction

Acyl and phosphoryl transfer reactions, in particular hydrolytic cleavage of carboxylic acid and phosphate esters, are of great biochemical and environmental importance. Metal ion catalysis in these reactions has been studied extensively during last decades both for the purposes of enzyme modeling and for development of artificial enzyme mimics [1]. Among different approaches to the interpretation of the role

of metal ions in catalysis, the direct binding of the catalyst (C) to the transition state of the uncatalyzed reaction (T^\ddagger) leading to the transition state of the catalytic reaction (CT^\ddagger) via an supposed pseudo-equilibrium (1) is of growing importance.



This approach currently plays a central role in the interpretation of enzyme catalysis [2–4] where it has served as a theoretical background for the development of transition state analog inhibitors [3–5] and catalytic antibodies [6]. It allows one to view the phenomenon of catalysis as a special type of molecular recognition where the enzyme active site serves as

* Fax: +52 55 56162010.

E-mail address: anatoli@servidor.unam.mx.

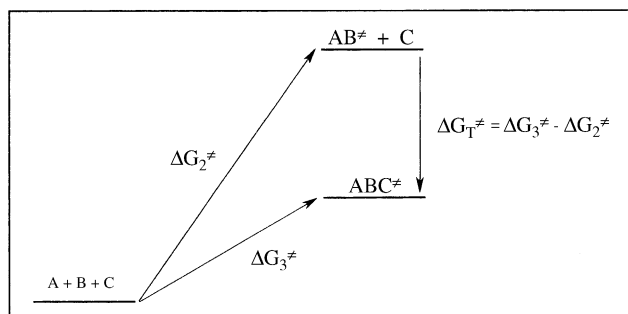


Fig. 1. The free energy diagram showing formation of the catalyst-transition state complex.

a receptor for the transition state of the uncatalyzed reaction [7]. Naturally, the concept has been extended successfully to interpretation of the supramolecular catalysis [7,8].

Transition state binding to the catalyst formalized as in Eq. (1) of course is not, and does not need to be, a process that really occurs. The situation is illustrated by thermodynamic cycles in Figs. 1 and 2 (see below), from which one can see that there are two real pseudo-equilibria leading to formation of transition states of uncatalyzed and catalytic reactions and this allows one to assign a free energy change and the respective equilibrium constant to the putative reaction (1) as far as the thermodynamic interpretation of transition state theory is valid. This methodology is essentially the same as that traditionally employed for discussion of medium effects on reaction rates [9]: a similar thermodynamic cycle is used to derive an expression for the free energy of transfer of the transition state from the reference medium to a medium of interest by using experimentally measurable transfer free energy of the substrate and reaction rates in both media. This free energy change is then converted to respective transition state activity or partition coefficients. In case of catalysis one also considers a “transfer” of the transition state from its form without the catalyst to its form involving the catalyst species, but it seems more appropriate to speak here about “binding” just because of the stoichiometric character of the process considered. In the limit of validity of the thermodynamic version of the transition state theory, the free energy change between levels of reactants and the highest transition

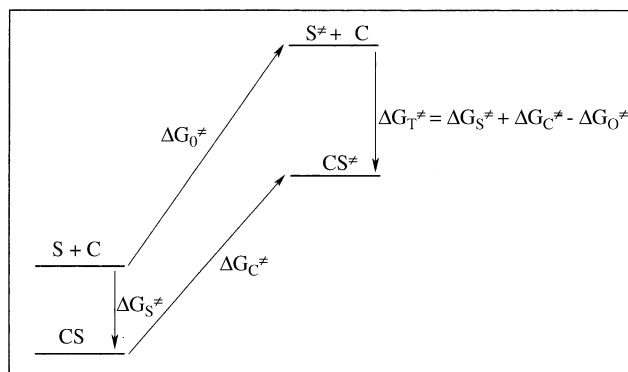


Fig. 2. The free energy diagram for a one-substrate catalytic reaction.

state is independent of the way in which the system reaches this transition state. So, there is no need to consider intermediates including catalyst-substrate complexes. Although the thermodynamic version of the transition state theory has some well known limitations resulting from the fact that it ignores the dynamic nature of the transition state, numerous successful applications of this methodology together with its relative simplicity make it still a very attractive approach.

In chemical catalysis, this approach was applied first to the analysis of acid and base catalyzed reactions and in these early studies the idea has been developed in a quantitative way. When the catalyst is H^+ or OH^- the equilibrium (1) refers to the direct protonation or deprotonation of the transition state. In other words, it allows one to consider transition states as acids or bases and to apply elaborated concepts of acid-base behavior of ground state molecules to the transition state and to kinetics [10]. Analysis of metal ion catalyzed reactions in terms of equilibrium (1) was performed first for metal ion promoted nucleophilic substitution in alkyl halides [11] and then this approach was extensively applied to acyl transfer reactions with crown ether derivatives in the presence of alkali and alkaline earth cations [12]. When the catalyst is a metal ion, the equilibrium (1) represents the direct complex formation of this ion with the transition state, which now can be viewed as a ligand and this treatment allows one to apply the concepts elaborated for analysis of stability of coordination compounds to reactivity and catalysis.

A qualitative discussion of direct transition state complexation in metal ion catalyzed phosphoryl and nucleotidyl transfer reactions were presented in a review article published ca. 30 years ago [13]. This paper reviews recent results on the kinetics of the metal ion catalyzed hydrolysis of carboxylic acid and phosphate esters in terms of transition state catalyst complexation providing constants for the pseudo-equilibrium (1) calculated for approximately 130 reactions. The literature of the last decade is mainly covered, but some relevant earlier results are also included.

2. Calculation of the binding constant of the catalyst to the transition state of the uncatalyzed reaction

Let us consider a chemical reaction between two substances A and B, which can proceed either in the absence or in the presence of a third substance C with the respective second-order and third-order rate constants k_2 and k_3 .



According to transition state theory the expressions for these rate constants can be written as

$$k_2 = \left(\frac{kT}{h} \right) \left(\frac{[AB^*]}{[A][B]} \right) \quad (4)$$

$$k_3 = \left(\frac{kT}{h} \right) \left(\frac{[ABC^\ddagger]}{[A][B][C]} \right) \quad (5)$$

where $[AB^\ddagger]$ and $[ABC^\ddagger]$ are the pseudo-equilibrium concentrations of the transition states for reactions (2) and (3), respectively. Now the ratio of rate constants k_3/k_2 takes the form:

$$\frac{k_3}{k_2} = \frac{[ABC^\ddagger]}{[AB^\ddagger][C]} \quad (6)$$

and apparently can be interpreted as the equilibrium constant K_T^\ddagger for the binding of C to the transition state AB^\ddagger as defined above in the Eq. (1):

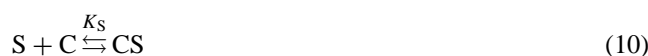
$$K_T^\ddagger (M^{-1}) = \frac{k_3}{k_2} = \exp \left(\frac{-\Delta G_T^\ddagger}{RT} \right) \quad (7)$$

where ΔG_T^\ddagger is the free energy of the binding of C to AB^\ddagger , which is related to activation free energies for reactions (2) and (3) by the Eq. (8). The situation is illustrated graphically in Fig. 1.

$$\Delta G_T^\ddagger = \Delta G_3^\ddagger - \Delta G_2^\ddagger \quad (8)$$

Although the above treatment is independent of the reaction mechanism, the transition state ABC^\ddagger indeed can be considered as a “coordination compound” between metal ion C and transition state AB^\ddagger only if the presence of C does not change the reaction mechanism, that is the structure of the fragment AB in the transition state ABC^\ddagger must be similar to the structure of AB^\ddagger . Therefore, this approach is limited by the cases when metal ion catalysis occurs due to such factors as Lewis acid activation of the substrate and/or nucleophile, template effect, leaving group stabilization, etc., but not due to formation of new covalent intermediates, as typically happens with organometallic catalytic systems.

The actual way to calculate K_T^\ddagger depends on the kinetic scheme of the catalytic reaction because for different kinetic schemes different parameters can be determined experimentally. The simplest case is the one-substrate reaction, which involves intermediate complex formation between substrate (S) and catalyst (C) in accordance with Eqs. (9)–(11):



Here, k_0 is the rate constant of uncatalyzed spontaneous transformation of the substrate, k_C the so-called catalytic rate constant of the transformation of catalyst–substrate complex CS and K_S is the stability constant of this complex. Often the reaction kinetics are studied at a fixed concentration of S and variable concentration of C taken in excess over concentration of S and parameters are calculated by fitting the observed

first-order reaction rate constant (k_{obs}) to the Eq. (12):

$$k_{\text{obs}} = \frac{k_0 + k_C K_S [C]}{1 + K_S [C]} \quad (12)$$

Applying the transition state theory formalism to this scheme one obtains:

$$k_0 = \left(\frac{kT}{h} \right) \left(\frac{[S^\ddagger]}{[S]} \right) \quad (13)$$

$$k_C K_S = \left(\frac{kT}{h} \right) \left(\frac{[CS^\ddagger]}{[C][S]} \right) \quad (14)$$

and the ratio $k_C K_S/k_0$ gives the required K_T^\ddagger value:

$$K_T^\ddagger = \frac{[CS^\ddagger]}{[S^\ddagger][C]} = \frac{k_C K_S}{k_0} \quad (15)$$

The respective free energy diagram is shown in Fig. 2.

It follows from the Eq. (15) that

$$k_C K_S = k_0 K_T^\ddagger \quad (16)$$

Combining Eqs. (12) and (16) one obtains [12]

$$k_{\text{obs}} = k_0 \left(\frac{1 + K_T^\ddagger [C]}{1 + K_S [C]} \right) \quad (17)$$

One can therefore calculate K_T^\ddagger directly from the experimental results by using the Eq. (17).

One important aspect in connection with this scheme is the fact that the catalytic effect expressed as k_C/k_0 can be related to the ratio of the binding constants of the substrate and the transition state to the catalyst:

$$\frac{k_C}{k_0} = \frac{K_T^\ddagger}{K_S} \quad (18)$$

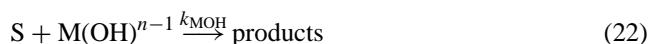
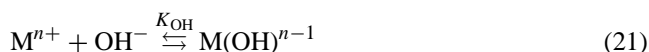
It becomes immediately evident from Eq. (18) as well as from (17) that a high catalytic effect requires the strongest possible binding of the catalyst to the transition state (largest possible K_T^\ddagger), but weakest possible binding to the substrate in the ground state (smallest possible K_S) in contrast to popular notion that the substrate–catalyst ground state complexation is important for catalysis and actually makes a catalyst “enzyme-like”.

If the reaction kinetics are studied at a fixed concentration of C and variable S, as is typical in enzyme kinetics, the classical Michaelis–Menten equation for the rate of the catalytic reaction is applied with $K_m = K_S^{-1}$ if the intermediate CS is in equilibrium with C and S:

$$-\frac{d[S]}{dt} = \frac{d[\text{product}]}{dt} = \frac{k_0[S] + k_C[C][S]}{K_m + [S]} \quad (19)$$

Note that according to Eq. (19) the reaction is still first-order in S only if $[S] \ll K_m$. Under these conditions, the value of K_m cannot be determined, but K_T^\ddagger can be calculated in accordance with Eq. (15).

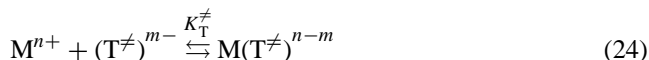
True one-substrate reactions are rare, however, and most often one deals with two-substrate reactions, e.g. in reactions discussed in this paper one substrate is an ester and the second substrate is a nucleophile. If one of the substrates has a negligible affinity to the catalyst the same treatment as for a one-substrate reaction can be applied with the only difference that k_0 and k_C will be now second-order rate constants for interactions of the first substrate in free and bound to catalyst forms with the second low-affinity substrate. This is the case for an important group of metal ion catalyzed reactions of alkaline hydrolysis of different substrates via formation of metal hydroxo complexes in accordance with Eqs. (20)–(22):



Here, M^{n+} is an aqua metal ion or a metal complex with at least one aqua ligand. The equation for K_T^\ddagger analogous to (15) has the form

$$K_T^\ddagger = \frac{k_{MOH} K_{OH}}{k_{OH}} \quad (23)$$

and refers to the equilibrium (24) where $(T^\ddagger)^{m-}$ is the transition state of the alkaline hydrolysis reaction.



To avoid confusion in terminology, although the term “catalyst” or “catalytically active form” is usually applied to the metal hydroxo complex, K_T^\ddagger refers to the transition state complexation with the respective aqua complex while OH^- forms part of the transition state $(T^\ddagger)^{m-}$ of the uncatalyzed reaction being one of the substrates.

Since the formation of hydroxo complexes is described as a rule in terms of dissociation of coordinated water with the respective pK_a value ($pK_a = 14 - \log K_{OH}$), a useful modification of the Eq. (23) is [14]

$$\log K_T^\ddagger = \log \left(\frac{k_{MOH}}{k_{OH}} \right) + 14 - pK_a \quad (25)$$

Reactions in which both substrates have significant affinity to the catalyst and the catalytic reaction proceeds via a distinctly detectable ternary complex between the catalyst

and both substrates, will not be discussed in this review. The respective equations can be found in references [3,4,8b,12].

3. Transition states for uncatalyzed hydrolyses of carboxylic acid and phosphate esters

With some exceptions the hydrolysis of carboxylic acid esters as well as di- and triesters of phosphoric acid proceeds via the addition–elimination mechanism illustrated for the alkaline hydrolysis of an ester in Fig. 3. The tetrahedral intermediate (pentacoordinated trigonal bipyramidal intermediate in case of phosphate esters) can be a very short-living species even non-existent in a limiting case of a concerted substitution mechanism. For substrates with good leaving groups, which are often used in kinetic experiments, the rate-determining step is usually the addition step.

Chart 1 shows the chemical structures of the substrates discussed in this review and Table 1 collects the rate constants for their uncatalyzed hydrolyses. For many of them, the available data allow one to calculate the acid dissociation constants of the transition states for the water hydrolysis (K_a^\ddagger), which are the conjugate acids for the transition states of the alkaline hydrolysis and serve therefore as an estimate of their basicity. Since the basicity of ligands often correlates with the stability of their metal complexes [15] it seems appropriate to take into account basicities of the transition state. For this reason, Table 1 also includes the respective K_a^\ddagger values, calculated in accordance with the Eq. (26) [10a].

$$pK_a^\ddagger = \log \left(\frac{k_{H_2O}}{k_{OH}} \right) + 14 \quad (26)$$

Fig. 4 illustrates the types of protolytic equilibria for transition states of carboxylic acid and phosphate esters. Note that in contrast to the behavior of “normal” organic acids, which become stronger in the presence of electron-withdrawing substituents, the transition states for substrates with leaving groups containing electron-withdrawing substituents are weaker acids than those with less activated leaving groups, e.g. the transition state for BDNPP is less acidic (higher pK_a^\ddagger) than that for BNPP. This trend reflects the fact that more activated substrates have earlier transition states with less bonding between carbonyl or phosphoryl group and the entering water molecule, which therefore becomes less acidified in the transition state.

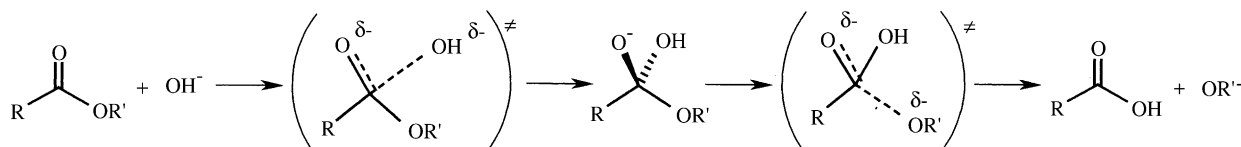


Fig. 3. The addition–elimination mechanism for ester hydrolysis.

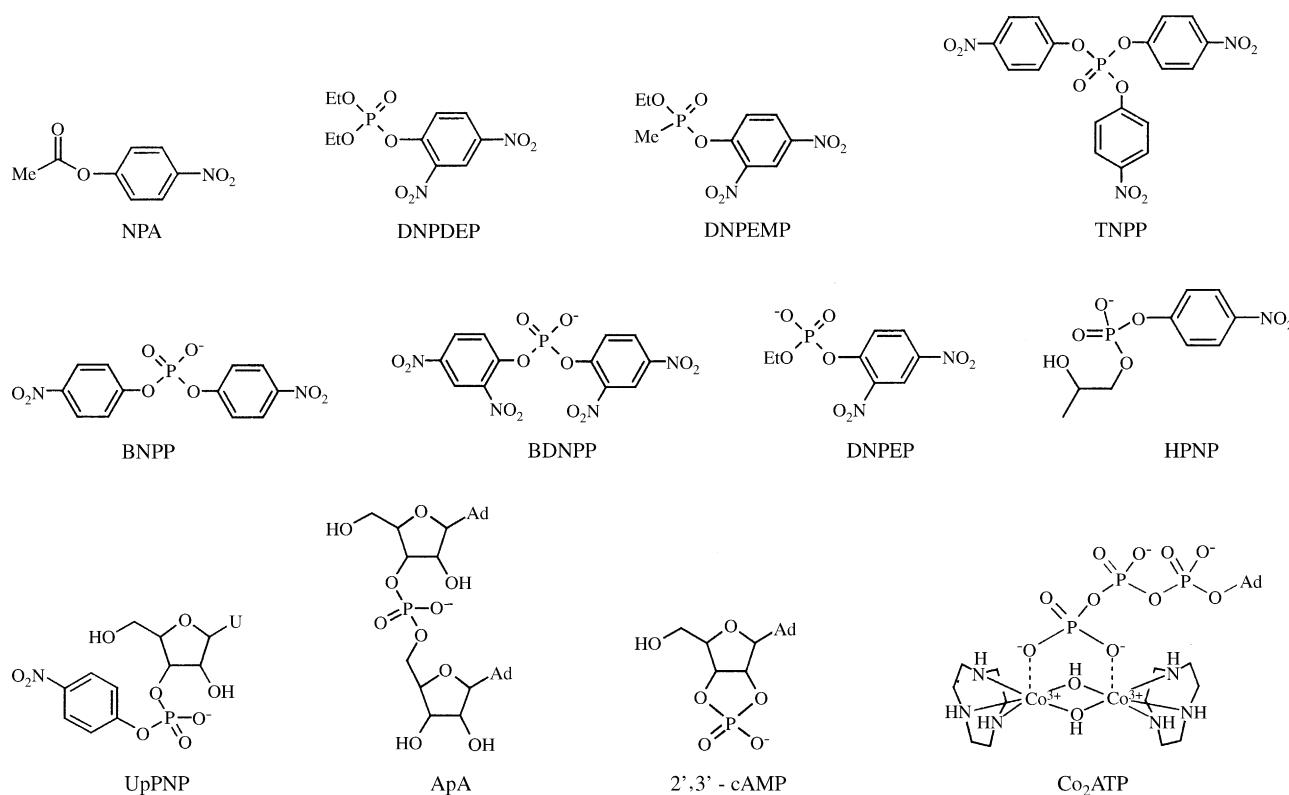


Chart 1. Chemical structures of substrates.

Table 1

Rate constants for alkaline (k_{OH}) and water ($k_{\text{H}_2\text{O}}$) hydrolyses of carboxylic acid and phosphate esters and $\text{p}K_{\text{a}}^{\ddagger}$ values (Eq. (26)) for transition states of uncatalyzed reactions

Substrate	k_{OH} ($\text{M}^{-1} \text{s}^{-1}$)	$k_{\text{H}_2\text{O}}$ (s^{-1})	T ($^{\circ}\text{C}$)	$\text{p}K_{\text{a}}^{\ddagger}$	Reference
NPA	14.8	5.5×10^{-7}	25	6.57	[16]
DNPDEP	0.305	1.22×10^{-6}	25	8.60	[17]
	0.565	2.26×10^{-6}	35		
DNPEMP	26.4	9.9×10^{-5}	25	8.57	[18]
	41.8	2.3×10^{-4}	35		
TNPP	10.7	1×10^{-3}	25	9.97	[19,20]
BNPP	5.8×10^{-6}	1.1×10^{-11}	25	8.30	[21,22]
	2.4×10^{-5}		35		[21b]
	$9.6 \times 10^{-5\text{a}}$	3×10^{-10}	50		[22]
BDNPP	3×10^{-3}	1.8×10^{-7}	25	9.8	[23]
DNPEP	$1 \times 10^{-4\text{b}}$		25		[24]
	8.4×10^{-4}	3.0×10^{-7}	39	10.55	[25] ^c
HPNP	0.1		25		[26]
UpPNP	1570		25		[26]
ApA	0.033		60		[27]
2',3'-cAMP	1.5×10^{-3}		30		[27]
	1.1×10^{-3}		25		[28]
Co ₂ ATP	0.027		25		[28]

^a Calculated with $E_{\text{a}} = 18.3 \text{ kcal/mol}$ [21a].

^b Approximate value.

^c 2,4-Dinitrophenyl methyl phosphate.

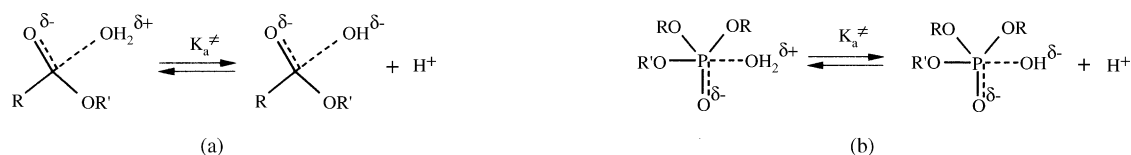


Fig. 4. Acid dissociation equilibria for transition states of water hydrolysis reactions of a carboxylic acid (a) and a phosphate (b) ester.

4. Transition state binding constants for catalytic hydrolyses

4.1. Carboxylic acid esters

The hydrolysis of NPA is a traditional test reaction for numerous biomimetic catalytic systems. It also has been a subject of extensive theoretical studies [30]. Table 2 contains rate constants for NPA hydrolysis by more than 30 metal hydroxo complexes, mainly Zn(II), with ligands shown in Chart 2. Transition state binding constants given in the fourth col-

Table 2

Rate constants, pK_a , values of coordinated water and transition state binding constants for the cleavage of NPA by metal complexes at 25 °C

Species	k_{MOH} ($\text{M}^{-1} \text{s}^{-1}$)	pK_a	$\log K_T^\ddagger$	Reference
[Co(1)OH] $^{2+}$	0.0093	6.3	4.5	[31]
[Co(NH $_3$) $_5$ OH] $^{2+}$	0.00152	6.4	3.61	
[Zn(2)OH] $^+$	0.1	7.9	3.93	[32]
[Zn(3)OH] $^+$	0.047	7.68	3.82	[33]
[Zn(4)OH] $^+$	0.036	7.3	4.09	[34]
[Zn(5)OH] $^+$	0.6	8.8	3.81	[35]
[Zn(6)OH]	0.089	8.05	3.73	[36]
[Zn(7a)OH]	1.15	7.1	5.79	[37]
[Zn(7b)OH]	1.08	7.4	5.46	
[Zn(7c)OH]	0.979	7.6	5.22	
[Zn(7d)OH]	1.09	7.3	5.57	
[Zn $_2$ (8a)(OH)] $^{3+}$	0.094	7.08	4.72	[38]
[Zn $_2$ (8a)(OH) $_2$] $^{2+}$	1.3	8.64	4.3	
[Zn $_2$ (8b)(OH)] $^{3+}$	1.16	7.52	4.51	
[Zn $_2$ (8b)(OH) $_2$] $^{2+}$	2.0	9.07	4.06	
[Zn $_2$ (8c)(OH)] $^{3+}$	0.35	7.85	4.52	
[Zn $_2$ (8c)(OH) $_2$] $^{2+}$	3.5	9.36	4.01	
[La(OH)] $^{2+}$	0.37	9.33	3.07	[14]
[Zn(9)OH] $^+$	0.71	8.0	3.7 ^a	[39] ^b
[Zn $_3$ (10)(OH) $_2$] $^{4+}$	0.56	8.57	4.01	[40]
[Zn $_3$ (10)(OH) $_3$] $^{3+}$	4.2	9.7	3.75	
[Zn $_3$ (11)(OH) $_2$] $^{4+}$	0.34	8.05	4.31	
[Zn $_3$ (11)(OH) $_3$] $^{3+}$	3.7	8.9	4.5	
[Zn $_3$ (12)(OH)] $^{5+}$	0.342	7.44	4.92	[41]
[Zn(13a)(OH)] $^+$	0.934	8.74	4.06	[42]
[Zn(13b)(OH)] $^+$	0.42	8.61	3.84	
[Zn(13c)(OH)] $^+$	0.36	8.60	3.79	
[Zn(13d)(OH)] $^+$	0.307	8.42	3.9	
[Zn(13e)(OH)] $^+$	0.256	8.43	3.81	
[Zn(13f)(OH)] $^+$	0.143	8.26	3.72	
[Zn(14)(OH)] $^+$	0.083	8.25	3.5 ^a	[43] ^c
[Co(14)(OH)] $^+$	0.241	8.52	3.7 ^a	
[Ni(14)(OH)] $^+$	0.285	8.58	3.7 ^a	
Zn(CA)(OH) d	400	7.0	8.4	[19]

^a Approximate value.

^b At 55 °C in 50% MeCN, $K_m = 7.6$ mM.

^c In 40% MeCN.

^d Bovine carbonic anhydrase.

umn of the Table 2 were calculated by using the Eq. (25) for a non-coordinating substrate. The pK_a values for the respective aqua complexes are also included.

Logarithms of transition state binding constants for the hydrolysis of NPA by Zn(II) complexes are plotted vs. logarithms of binding constants of hydroxo anion ($\log K_{\text{OH}} = 14 - pK_a$) in Fig. 5. All points lay below the dashed line, which corresponds to $K_T^\ddagger = K_{\text{OH}}$. Obviously, the transition state binding for all complexes is weaker than the ground state binding of a coordinating substrate. With other metal ions (La(III), Co(III) and Ni(II)) in Table 2 the situation is similar. Therefore, the question is why is catalysis observed at all? The usual answer is that the reason for catalysis is the “nucleophile activation”, that is generation of coordinated OH anions by acidification of metal bound water molecules at low pH values where the autoprotolysis of bulk water produces a very small concentration of OH $^-$. This is therefore the ground state rather than the transition state effect. In terms of transition state binding the situation may be described differently. The contribution of the catalytic reaction to the observed rate constant for the ester hydrolysis in the presence of a metal hydroxo complex equals

$$k_{\text{cat}} = k_{\text{MOH}}[\text{MOH}] = k_{\text{MOH}}K_{\text{OH}}[\text{M}][\text{OH}^-] \quad (27)$$

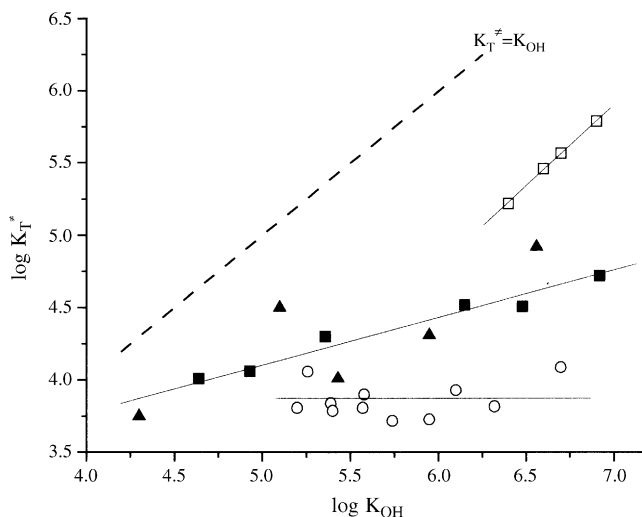


Fig. 5. Logarithms of transition state binding constants for the hydrolysis of NPA by Zn(II) complexes vs. logarithms of binding constants of hydroxo anion. Open squares: mononuclear complexes with finger peptides; open circles: mononuclear complex with other ligands; solid squares: binuclear complexes with macrocyclic ligands; solid triangles: trinuclear complexes. Dashed line corresponds to $K_T^\ddagger = K_{\text{OH}}$.

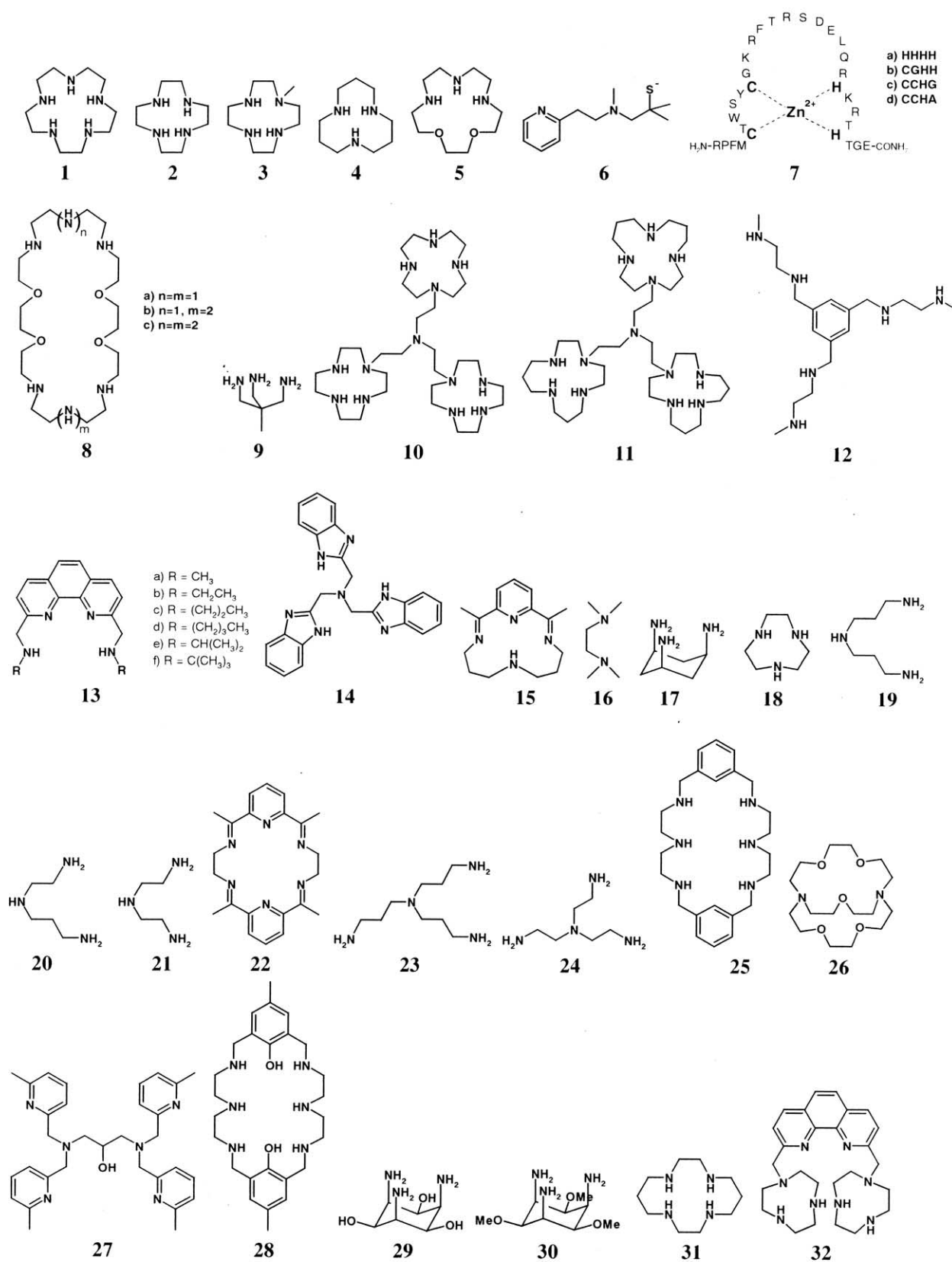


Chart 2. Chemical structures of ligands.

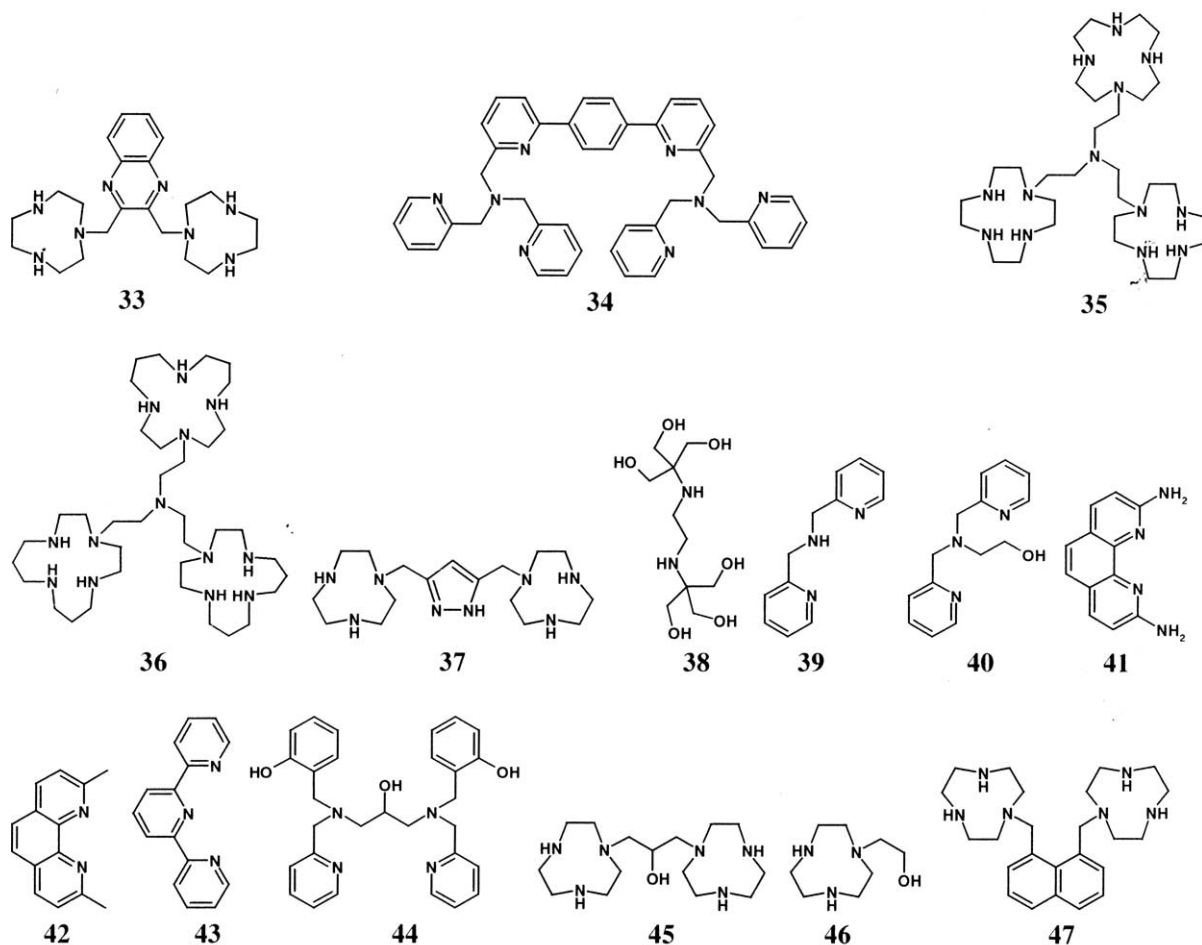


Chart 2. (Continued).

and the contribution of the non-catalyzed hydrolysis is

$$k_{\text{non}} = k_{\text{OH}}[\text{OH}^-] \quad (28)$$

Therefore, the catalytic effect $k_{\text{cat}}/k_{\text{non}}$ at a given pH value equals

$$\frac{k_{\text{cat}}}{k_{\text{non}}} = \frac{k_{\text{MOH}}K_{\text{OH}}[\text{M}]}{k_{\text{OH}}} = K_{\text{T}}^{\ddagger}[\text{M}] \quad (29)$$

It follows from Eq. (29) that the observed catalytic effect as a matter of fact is independent of the ground state binding and is proportional to the transition state binding constant and the metal complex concentration. At pH below $\text{p}K_{\text{a}}$ of the metal aqua complex $[\text{M}]$ equals the total metal concentration and under these conditions with an average K_{T}^{\ddagger} value of ca. 10^4 M^{-1} (Table 2) the reaction rate will increase by an order of magnitude in the presence of just 1 mM metal complex. Let us consider now the values of K_{T}^{\ddagger} .

Inspection of Fig. 5 shows that, in general, there is no correlation between K_{T}^{\ddagger} and K_{OH} values. However, when groups of structurally related complexes are considered separately a certain correlation within each group of complexes

is clearly seen. Open circles show results for mononuclear complexes with ligands 2–6 and 13a–f. They lie on a horizontal line, which means that within this series of complexes the factors favoring the hydroxide binding do not affect the transition state binding. Probably, in these complexes, Zn(II) always has just one coordination site available for hydroxide and transition state binding and therefore binds only the attacking hydroxide in both states. Solid squares show the results for binuclear complexes with macrocyclic ligands 8a–c. Here, a positive slope of 0.35 is clearly seen indicating that stronger binding of hydroxide is also accompanied by stronger transition state binding. Results for trinuclear complexes (solid triangles) with ligands 10–12 are generally close to the regression line drawn through points for binuclear complexes with the exception of two species $[\text{Zn}_3(\mathbf{11})(\text{OH})_3]^{3+}$ and $[\text{Zn}_3(\mathbf{12})(\text{OH})]^{5+}$ which show some positive deviations attributable to better preorganization of the polynuclear complexes for transition state binding. Results for mononuclear complexes with finger peptides 7a–d (open squares) form a line with unit slope indicating a similar increase in affinity toward ground and transition states upon variation on the complex structure. In the structure 7 (Chart 2), amino acid

residues presented by bold letters are those which are coordinated to Zn(II). The wild type peptide with two cysteine and two histidine residues forms an inactive complex, but mutations of the residues presented by sequences **a–d** produce peptides which have lower coordinating power, but high catalytic activity in NPA hydrolysis.

The ideal structural variation would give a better transition state binding without affecting the ground state binding, which would be represented by a vertical line in Fig. 5. Obviously, no system approaches this tendency and it is still unclear which structural features must be implemented in the ligand to afford strong transition state complexation. The last line in Table 2 gives the results for NPA hydrolysis by bovine carbonic anhydrase, a Zn(II) enzyme, which catalyzes CO₂ hydration. It shows a very significant positive deviation from all synthetic catalysts and is the only catalyst for which $\log K_T^\ddagger = 8.4$ surpasses $\log K_{OH} = 7.0$. NPA is not a specific substrate for carbonic anhydrase. This enzyme does not possess an optimum structure for the esterolytic function at all and has rather a modest reactivity toward NPA cleavage by biological standards, e.g. NPA cleavage by human serum albumin proceeds two orders of magnitude faster (second-order rate constant $3 \times 10^4 \text{ M}^{-1} \text{ s}^{-1}$ [44]).

Let us discuss now the absolute values of K_T^\ddagger . Being lower than K_{OH} they are nevertheless surprisingly large taking into account the transition state structure for NPA hydrolysis (Fig. 4a). Phosphonate and phosphodiester monoanions are widely used as transition state analogs for alkaline hydrolysis of aryl esters [6,30], but they form very unstable complexes with Zn(II) with $\log K$ below 0.5 [19]. However, the transition state for NPA hydrolysis is much more basic than these anions and therefore may be a better ligand. Table 3 collects stability constants for complexes of $[\text{Zn}(\mathbf{4})]^{2+}$ with transition states of alkaline hydrolysis of different substrates and with some anionic ligands. One can see from these data that, first, more basic ligands including transition states do form more stable complexes and, second, that the transition state for NPA hydrolysis is close by its basicity to bicarbonate anion and both ligands have similar affinity to $[\text{Zn}(\mathbf{4})]^{2+}$ with $\log K$ about 4.

Table 3

Stability constants for complexes of $[\text{Zn}(\mathbf{4})]^{2+}$ with transition states of the alkaline hydrolysis of different substrates and with some anionic ligands [19]

Substrate	$\text{p}K_a^\ddagger$	$\log K_T^\ddagger$
CH ₃ COOCH ₃	5.22	4.07
NPA	6.57	4.09
BNPP	8.3	7.25
TNPP	9.97	6.52

Ligand	$\text{p}K_a$	$\log K$
(PhO) ₂ PO ₂ [−]	1.85	<0.5
CH ₃ COO [−]	4.76	2.6
4-O ₂ N-C ₆ H ₄ OPO ₃ ^{2−}	5.09	3.1
PhOPO ₃ ^{2−}	5.8	3.5
HCO ₃ [−]	6.35	4.0
OH [−]	15.7	6.7

The binding constants of all ligands to $[\text{Zn}(\mathbf{4})]^{2+}$ are approximately two orders of magnitude larger than to Zn(II) aqua ion due to a combination of several yet poorly understood factors and this difference apparently exists for the transition state binding as well, because the aqua ion does not catalyze NPA hydrolysis [19].

Another factor, which may contribute to stronger transition state binding is possible bidentate coordination schematically shown in Fig. 6a–c for different types of substrates. Such bidentate coordination, which requires formation of a four-membered chelate cycle, is repeatedly proposed for ligands like carboxylates and phosphates, but is considered rather improbable in solution [45]. The situation may be quite different for transition states, however. Fig. 7 shows the simulated structure of the transition state for the alkaline hydrolysis of NPA, from which one can see that the distance between entering OH[−] and carbonyl carbon is about twice as large as the length of the covalent bond. As a result the distance between carbonyl oxygen and entering hydroxo anion also becomes large (Fig. 6d). Both oxygen donor atoms become positioned at a distance closer to the distance between oxygen atoms of ligands like glycolate, oxalate or catecholate

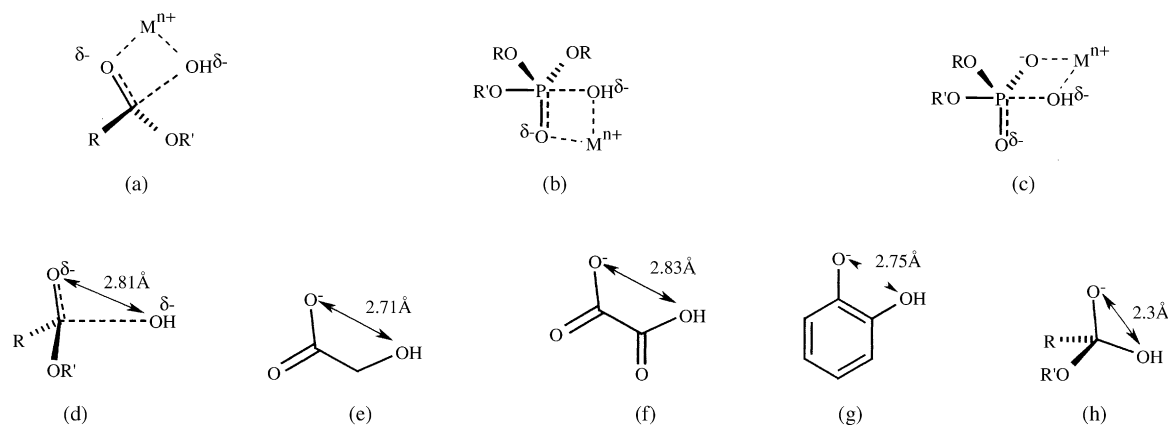


Fig. 6. Bidentate coordination of transition states for alkaline hydrolysis (a–c) and distances between oxygen atoms in the transition state of NPA hydrolysis (d), model ligands (e–g) and the tetrahedral intermediate of the NPA hydrolysis (h).

Considering groups of related complexes one observes rather scattered correlations between $\log K_T^\ddagger$ and $\log K_{OH}$ within each group with positive slopes 1.4 for Cu(II) complexes (solid squares) and 2.75 for Co(III) complexes (solid triangles). The slopes above unity indicate that structural modifications of the ligands induce larger increase in the transition state than in the ground state complexation. The conformational role of ligands in the series of Co(III) complexes, which show especially high positive slope is discussed in ref. [22] in connection with hydrolysis of BNPP (see below).

4.3. Phosphate diesters

Catalytic hydrolysis of BNPP has been studied extensively as a model process for hydrolysis of DNA. Results for this substrate are collected in Table 5 and related results for more activated phosphate diesters BDNPP and DNPEP are given in Tables 6 and 7. Fig. 9 illustrates the relationship between transition and ground state binding for BNPP. Comparing it to Figs. 5 and 8, which show related data for NPA and DNPDEP, one may clearly see a gradual shift in the type of distribution of points around the line corresponding to $K_T^\ddagger = K_{OH}$: for the carboxylic acid ester all points are below the line, for the phosphate trimester, points are distributed around the line and for the phosphate diester, all points are above the line. With two other phosphate diesters BDNPP and DNPEP, although less extensively studied, the situation is similar to BNPP: as is evident from Tables 6 and 7 the values of $\log K_T^\ddagger$ are larger than $\log K_{OH}$ for practically all metal complexes. The ground state hydroxide complexation is similar in all cases and, therefore, this tendency indicates increased transition state complexation. Partly, this may be attributed to

increased basicity of transition states for phosphate ester hydrolysis (see Table 1), but the principal effect seems to be the increased bidentate coordination in accordance with structures shown in Fig. 6a and b. From this point of view, the increased transition state binding reflects increased basicity in the order $C=O < P=O < P-O^-$. The magnitude of this effect is, however, very much different for different metal ions. Thus, for Zn(II) complexes with $\log K_{OH}$ about 6 (pK_a about 8) the values of $\log K_T^\ddagger$ are in the range 4–4.5 for NPA and in the range 6–7 for BNPP, but for La(III) $\log K_T^\ddagger$ increases from 3 for NPA to 9 for BNPP. Such enormous increase in affinity to La(III) is difficult to interpret at the moment.

Let us consider the tendencies within different groups of complexes in Fig. 9. Results for binuclear Zn(II) complexes (solid squares) show a linear dependence with a unit slope from which only one point for $[Zn_2(33)(OH)_3]^+$ deviates positively. The elevated reactivity of this complex was attributed to a favorable preorganization of the complex for accommodation of the substrate before the nucleophilic attack by one of coordinated hydroxide anions [57]. Results for mononuclear (open circles) and trinuclear (solid triangles) Zn(II) complexes follow essentially the same line.

Results for complexes with other metals are too limited for a meaningful correlation, but qualitatively there is an impression that for each metal cation a similar trend with a unit slope is observed, each line being shifted to higher transition state binding in the order $Zn(II) < Cu(II) < Ni(II) < Ln(III)$. Results for Co(III) (last three lines in Table 5, not shown in Fig. 9) follow the line for Ln(III). The absolute values of K_T^\ddagger for lanthanide(III) cations are very large. Considering as transition state analogs, ligands shown in Fig. 6e–g, and taking into account that the transition state of BNPP hydrolysis is a dianion, one can compare $\log K_T^\ddagger = 9.32$ for La(III) (Table 5) with the stability constant of catecholate complex of La(III) $\log K = 9.46$ [64]. However, stabilities of catecholate complexes with Zn(II) and Ni(II) are of the same order of magnitude and with Cu(II) $\log K = 13.9$. Therefore, the specificity of lanthanides as catalysts for phosphodiester hydrolyses requires special consideration. One essential factor is the large coordination number of these cations and low directionality of bonding, which allow the optimum fit of the metal ion to the transition state [1h].

Another phosphodiester, which attracts considerable interest as a model for RNA hydrolysis is HPNP. Results for this substrate are given in Table 8, which also lists the $\log K_{OH}$ values. Interestingly, with this substrate the values of $\log K_T^\ddagger$ are generally close to $\log K_{OH}$, as was the case for phosphate triesters. The cleavage of this substrate does not involve direct nucleophilic attack by coordinated hydroxide, which participates as a base for deprotonation of the substrate alcohol group serving as the intramolecular nucleophile [1n]. The values of K_T^\ddagger for the same Zn(II) complexes are ca. one order of magnitude smaller for HPNP than for BNPP (cf. Tables 5 and 8). This may reflect a weaker interaction of the metal ion with entering alkoxo nucleophile in the transition

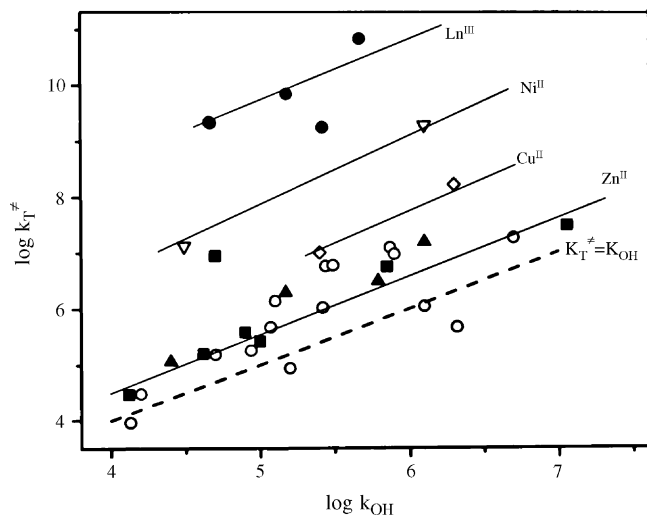


Fig. 9. Logarithms of transition state binding constants for the hydrolysis of BNPP by metal complexes vs. logarithms of binding constants of hydroxide anion. Open circles: mononuclear Zn(II) complexes; solid squares: binuclear Zn(II) complexes; solid triangles: trinuclear Zn(II) complex; open diamonds: binuclear Cu(II) complexes; open triangles: binuclear Ni(II) complexes; solid circles: Ln(III) complexes. Dashed line corresponds to $K_T^\ddagger = K_{OH}$.

Table 5

Rate constants and transition state binding constants for the cleavage of BNPP by metal complexes

Species	<i>T</i> (°C)	<i>k</i> _{MOH} (M ⁻¹ s ⁻¹)	p <i>K</i> _a	log <i>K</i> _T [‡]	Reference
[Zn(2)OH] ⁺	35	2.1 × 10 ⁻⁵	7.9	6.04	[51]
[Zn(3)OH] ⁺	35	5.2 × 10 ⁻⁶	7.68	5.66	
[Zn(4)OH] ⁺	35	8.5 × 10 ⁻⁵	7.3	7.25	
[Zn(5)OH] ⁺	35	1.31 × 10 ⁻⁵	8.8	4.94	[35]
[Zn(25)OH] ⁺	35	5 × 10 ⁻⁵	9.06	5.26	[52]
[Zn ₂ (25)OH] ³⁺	35	6 × 10 ⁻⁶	6.94	7.46	
[Zn ₂ (8a)(OH) ₂] ²⁺	35	1.15 × 10 ⁻⁴	9.1	5.58	[38]
[Zn ₂ (8b)(OH) ₂] ²⁺	35	9.08 × 10 ⁻⁵	9.38	5.2	
[Zn ₂ (8c)(OH) ₂] ²⁺	35	5.4 × 10 ⁻⁵	9.88	4.47	
[Eu(26)OH] ²⁺	50	0.4	7.8	9.9 ^a	[53]
[Ni ₂ (27-H ₋₁)OH] ²⁺	35	0.035	7.9	9.26	[54]
[CuCd(28)OH] ⁺	35	0.015	7.8	9.0 ^a	[55] ^b
[Zn(17)OH] ⁺	25	9.7 × 10 ⁻⁵	8.13	7.09	[56]
[Zn(29)OH] ⁺	25	1.2 × 10 ⁻⁴	8.56	6.76	
[Zn(30)OH] ⁺	25	1.1 × 10 ⁻⁴	8.51	6.77	
[Zn(18)OH] ⁺	25	6.8 × 10 ⁻⁵	8.1	6.97	
[Zn(21)OH] ⁺	25	2.3 × 10 ⁻⁵	8.93	5.67	
[Zn(20)OH] ⁺	25	6.4 × 10 ⁻⁵	8.90	6.14	
[Zn(19)OH] ⁺	25	2.3 × 10 ⁻⁵	8.58	6.02	
[Zn(31)OH] ⁺	25	3.9 × 10 ⁻⁶	9.87	3.96	
[Zn(24)OH] ⁺	25	1.1 × 10 ⁻⁵	9.8	4.48	
[Zn(32)(OH)] ⁺	35	7.5 × 10 ⁻⁵	9.3	5.19	[57]
[Zn ₂ (32)(OH) ₂]	35	6.9 × 10 ⁻⁵	10.7	3.76	
[Zn ₂ (32)(OH) ₃] ⁺	35	6.3 × 10 ⁻⁵	9.0	5.42	
[Zn ₂ (33)(OH) ₃] ⁺	35	4.2 × 10 ⁻³	9.3	6.94	
[Cu ₂ (34)OH] ³⁺	55	8.3 × 10 ⁻³	7.7	8.2 ^a	[58] ^c
[Cu ₂ (34)(OH) ₂] ²⁺	55	3.8 × 10 ⁻³	8.6	7.0	
[Zn ₃ (35)(OH) ₂] ⁴⁺	35	1.2 × 10 ⁻⁴	8.21	6.49	[40]
[Zn ₃ (35)(OH) ₃] ³⁺	35	1.1 × 10 ⁻⁴	9.6	5.06	
[Zn ₃ (36)(OH) ₂] ⁴⁺	35	2.9 × 10 ⁻⁴	7.90	7.18	
[Zn ₃ (36)(OH) ₃] ³⁺	35	3.1 × 10 ⁻⁴	8.83	6.28	
[Zn ₂ (37-H ₋₁)(OH)] ²⁺	35	1.87 × 10 ⁻⁴	8.15	6.74	[59]
[Ni ₂ (37-H ₋₁)(OH)] ²⁺	35	1.00 × 10 ⁻²	9.51	7.12	
[La(OH)] ²⁺	25	0.26	9.33	9.32	[14]
[Pr(OH)] ²⁺	25	0.26	8.82	9.83	
[Eu(OH)] ²⁺	25	0.038	8.58	9.24	
[Dy(OH)] ²⁺	25	0.81	8.33	10.82	
[La ₂ (38) ₂ (OH) ₅] ⁺	25	0.275	9.34	9.33	
[Co(2)OH] ²⁺	50	0.46	5.6	12.08	[22]
[Co(24)OH] ²⁺	50	0.081	5.5	10.43	
[Co(23)OH] ²⁺	50	2.5	4.8	13.62	

^a Approximate value.^b 75% EtOH.^c 30% DMSO.

Table 6

Rate constants and transition state binding constants for the cleavage of BDNPP by metal complexes

Species	<i>T</i> (°C)	<i>k</i> _{MOH} (M ⁻¹ s ⁻¹)	p <i>K</i> _a	log <i>K</i> _T [‡]	log <i>K</i> _{OH}	Reference
[Cu(39)OH] ⁺	25	0.03	9.0	6	5.0	[60]
[Cu(40)OH] ⁺		0.014	8.9	5.77	5.1	
[Cu(41)OH] ⁺		20	5.5	12.32	8.5	[61]
[Cu(42)OH] ⁺		0.8	7.0	9.43	7	
[Cu(43)OH] ⁺		5.7 × 10 ⁻⁴	8.2	5.08	5.8	
[Cu ₂ (44-H ₋₁)](AcO)OH] ⁺	50 ^a	0.045	5.9	8.19	8.1	[62]
Fe ₂ O(Phen) ₄ (OH) ³⁺	50	6.1	5.0	11.31	9.0	[63]

^a 25% MeOH.

Table 7

Rate constants and transition state binding constants for the cleavage of DNPEP by metal complexes at 25 °C [24]

Species	k_{MOH} ($\text{M}^{-1} \text{s}^{-1}$)	$\text{p}K_{\text{a}}$	$\log K_{\text{T}}^{\ddagger}$	$\log K_{\text{OH}}$
[Cu(17)OH] ⁺	0.0256	8.2	8.21	5.8
[Cu(4)OH] ⁺	0.231	8.4	8.96	5.6
[Cu(18)OH] ⁺	0.0118	7.7	8.37	6.3
[Cu(19)OH] ⁺	5×10^{-4}	9.6	5.10	4.4
[Cu(20)OH] ⁺	2×10^{-4}	9.5	4.80	4.5
[Cu(21)OH] ⁺	6×10^{-4}	9.1	5.68	4.9

Table 8

Rate constants and transition state binding constants for the cleavage of HPNP by metal complexes at 25 °C

Species	k_{MOH} ($\text{M}^{-1} \text{s}^{-1}$)	$\text{p}K_{\text{a}}$	$\log K_{\text{T}}^{\ddagger}$	$\log K_{\text{OH}}$	Reference
[Zn(17)OH] ⁺	0.12	8.13	5.95	5.87	[56]
[Zn(29)OH] ⁺	0.23	8.56	5.8	5.44	
[Zn(30)OH] ⁺	0.17	8.51	5.72	5.49	
[Zn(18)OH] ⁺	0.065	8.1	5.71	5.9	
[Zn(21)OH] ⁺	0.12	8.93	5.15	5.07	
[Zn(20)OH] ⁺	0.13	8.90	5.21	5.1	[65]
[Zn(19)OH] ⁺	0.02	8.58	4.72	5.42	
[Zn(4)OH] ⁺	0.018	7.44	5.81	6.56	
[Zn ₂ (45-H ₋₁)OH] ²⁺	0.71	7.8	7.05	6.2	
[Zn(46)OH] ⁺	0.061	9.2	4.58	4.8	
[Cd ₂ (45)OH] ²⁺	4.0	9.0	6.6	5.0	[66]

Table 9

Rate constants and transition state binding constants for the cleavage of different substrates by metal complexes

Substrate	Species	T (°C)	k_{MOH} ($\text{M}^{-1} \text{s}^{-1}$)	$\text{p}K_{\text{a}}$	$\log K_{\text{T}}^{\ddagger}$	$\log K_{\text{OH}}$	Reference
UpPNP	[Zn ₂ (45-H ₋₁)OH] ²⁺	25	203	7.8	5.31	6.2	[26]
ApA	[Cu ₂ (47)OH] ³⁺	50	0.59	6.1	9.1 ^a	7.9	
2',3'-cAMP	[Cu ₂ (47)OH] ³⁺	25	3.4	6.0	11.5	8.0	[67]
2',3'-cAMP	[Cu(trpy)OH] ⁺	37	1.4×10^{-2}	8.08	6.7 ^b	5.92	
Co ₂ ATP	Mg ²⁺	25	229 ^c		3.93		[29]
2',3'-cAMP	[Cu(41)OH] ⁺	25	38	5.5	13.04	8.5	[27]
2',3'-cAMP	[Cu(42)OH] ⁺		0.062	7.0	8.75	7.0	
2',3'-cAMP	[Cu(43)OH] ⁺		5.1×10^{-3}	8.2	6.47	5.8	

^a At 60 °C.^b Approximate value.^c The third-order rate constant ($\text{M}^{-2} \text{s}^{-1}$), $K_{\text{m}} = 0.35 \text{ M}$.

state of HPNP cleavage than with entering hydroxo anion in BNPP hydrolysis.

Table 9 shows $\log K_{\text{T}}^{\ddagger}$ values for several other different substrates. The most impressive is a very large value of $K_{\text{T}}^{\ddagger} = 10^{13} \text{ M}^{-1}$ for the hydrolysis of 2',3'-cAMP by Cu(41)²⁺. Strong transition state stabilization was attributed to hydrogen bonding of the anionic transition state to terminal amino groups of the ligand [27]. The complex with ligand 42 lacking these amino groups binds the transition state ca. four orders of magnitude weaker, but the stabilizing effect of amino groups on the ground state hydroxide binding is much smaller: $\Delta \log K_{\text{OH}} = 1.5$ (Table 9). Apparently, the amino groups are properly positioned for preferable recognition of the transition state.

Hydrolysis of Co₂ATP in the presence of Mg(II) nearly perfectly fits the simplest scheme represented by reactions (2) and (3) for non-coordinating substrates. The transition state binding constant for Mg(II) is close to the stability constant

for Mg(II) complex with ADP³⁻ ($\log K = 3.17$) in accordance with the proposed [29] associative hydrolysis mechanism.

5. Conclusions

This review provides the first extensive compilation of transition state binding constants for a large number of metal complex catalysts and substrates. Only general trends in K_{T}^{\ddagger} values have been discussed with an emphasis on interrelationships between the ground state and transition state complexation, which revealed some mechanistically useful patterns in series of different substrates and/or different metals. Viewing transition states as ligands requires considering as transition state analogs some species, which are different from those generally accepted on the basis of only structural and charge similarity. In addition, the “nucleophile activation” was shown to be attributable to transition state stabilization.

Of course, not all catalytic systems can be discussed in terms of this approach because the required kinetic parameters are not always available. In particular, the stability constant for the catalyst–nucleophile complex required to transform the experimentally measured second-order rate constant for the reaction between the catalyst active form and the substrate into the third-order rate constant for the reaction between free nucleophile, free metal complex and the substrate cannot always be determined. Nevertheless, the number of reactions to which this approach is applicable is large enough to expect some interesting generalizations in the future.

Acknowledgements

The author thanks Anthony J. Kirby for helpful and stimulating discussions and the Royal Society for awarding the RSC Journals Grant, which provided support for this work.

References

- [1] For recent reviews see;
 - (a) E. Kimura, T. Koike, *Adv. Inorg. Chem.* 44 (1997) 229;
 - (b) J. Chin, *Curr. Opin. Chem. Biol.* 1 (1997) 514;
 - (c) E.L. Hegg, J.N. Burstyn, *Coord. Chem. Rev.* 173 (1998) 133;
 - (d) B.N. Trawick, A.T. Daniher, J.K. Bashkin, *Chem. Rev.* 98 (1998) 939;
 - (e) M. Komiyama, J. Sumaoka, *Curr. Opin. Chem. Biol.* 2 (1998) 751;
 - (f) N.H. Williams, B. Takasaki, M. Wall, J. Chin, *Acc. Chem. Res.* 32 (1999) 485;
 - (g) R. Kramer, *Coord. Chem. Rev.* 182 (1999) 243;
 - (h) A. Blasko, T.C. Bruice, *Acc. Chem. Res.* 32 (1999) 475;
 - (i) P. Molenveld, J.F.J. Engbersen, D.N. Reinhoudt, *Chem. Soc. Rev.* 29 (2000) 75;
 - (j) S.J. Franklin, *Curr. Opin. Chem. Biol.* 5 (2001) 208;
 - (k) H.-J. Schneider, A.K. Yatsimirsky, in: A. Sigel, H. Sigel (Eds.), *Metal Ions in Biological Systems*, vol. 40, M. Dekker, Inc., New York/Basel, 2003, p. 369;
 - (l) N.H. Williams, *Biochim. Biophys. Acta* 1697 (2004) 279;
 - (m) C.L. Liu, M. Wang, T.L. Zhang, H.Z. Sun, *Coord. Chem. Rev.* 248 (2004) 147;
 - (n) J.R. Morrow, O. Iranzo, *Curr. Opin. Chem. Biol.* 8 (2004) 192.
- [2] T.C. Bruice, S.J. Benkovic, *Biochemistry* 39 (2000) 6267.
- [3] R. Wolfenden, *Acc. Chem. Res.* vol. 5 (1972) 10.
- [4] G.E. Lienhard, *Science* 180 (1973) 149.
- [5] M.M. Mader, P.A. Bartlett, *Chem. Rev.* 97 (1997) 1281.
- [6] (a) R.A. Lerner, S.J. Benkovic, P.G. Schultz, *Science* 252 (1991) 659;
- (b) J.D. Stewart, S.J. Benkovic, *Chem. Soc. Rev.* 21 (1993) 213.
- [7] A.J. Kirby, *Angew. Chem. Int. Ed. Engl.* 35 (1996) 707.
- [8] (a) O.S. Tee, *Adv. Phys. Org. Chem.* 29 (1994) 1;
- (b) H.-J. Schneider, A.K. Yatsimirsky, *Principles and Methods in Supramolecular Chemistry*, John Wiley & Sons Ltd., Chichester, UK, 2000, p. 301.
- [9] E. Buncel, H. Wilson, *Acc. Chem. Res.* 12 (1979) 42.
- [10] (a) J.L. Kurz, *Acc. Chem. Res.* 5 (1972) 1;
- (b) J.L. Kurz, *J. Am. Chem. Soc.* 85 (1963) 987.
- [11] E.S. Rudakov, I.V. Kozhevnikov, V.V. Zamaschikov, *Russ. Chem. Rev. Engl. Trans.* 43 (1974) 305.
- [12] (a) R. Cacciapaglia, A.R. van Doorn, L. Mandolini, D.N. Reinhoudt, W. Verboom, *J. Am. Chem. Soc.* 114 (1992) 2611;
- (b) R. Cacciapaglia, L. Mandolini, *Chem. Soc. Rev.* 22 (1993) 221.
- [13] B.S. Cooperman, in: H. Sigel (Ed.), *Metal Ions in Biological Systems*, 5, M. Dekker, Inc., New York, 1976, p. 80.
- [14] P. Gómez-Tagle, A.K. Yatsimirsky, *Inorg. Chem.* 40 (2001) 3786.
- [15] R.N. Martin, H. Sigel, *Comments Inorg. Chem.* 6 (1988) 285.
- [16] (a) D.J. Hupe, W.P. Jencks, *J. Am. Chem. Soc.* 99 (1977) 451;
- (b) W.P. Jencks, J. Carriuolo, *J. Am. Chem. Soc.* 82 (1960) 1778.
- [17] R.W. Hay, N. Govan, *Polyhedron* 16 (1997) 4233.
- [18] R.W. Hay, N. Govan, P.R. Norman, *Transition Met. Chem.* 23 (1998) 133.
- [19] E. Kimura, in: K.D. Karlin (Ed.), *Progress in Inorganic Chemistry*, vol. 41, 1994, p. 443.
- [20] J.R. Cox Jr., O.B. Ramsay, *Chem. Rev.* 64 (1964) 317.
- [21] (a) J.A.A. Ketelaar, H.R. Gersmann, *Rec. Trav. Chim.* 77 (1958) 973;
- (b) T. Koike, E. Kimura, *J. Am. Chem. Soc.* 113 (1991) 8935.
- [22] J. Chin, M. Banaszczuk, V. Jubian, X. Zou, *J. Am. Chem. Soc.* 111 (1989) 186.
- [23] C.A. Bunton, S.J. Farber, *J. Org. Chem.* 34 (1969) 767.
- [24] T. Itoh, H. Hisada, Y. Usui, Y. Fujii, *Inorg. Chim. Acta* 283 (1998) 51.
- [25] A.J. Kirby, M. Younas, *J. Chem. Soc. B* (1970) 1165.
- [26] M. Yang, J.P. Richard, J.R. Morrow, *Chem. Commun.* (2003) 2832.
- [27] M.J. Young, J. Chin, *J. Am. Chem. Soc.* 117 (1995) 10577.
- [28] M. Wall, B. Linkletter, D. Williams, A. Lebus, R.C. Hynes, J. Chin, *J. Am. Chem. Soc.* 121 (1999) 4710.
- [29] N.H. Williams, *J. Am. Chem. Soc.* 122 (2000) 12023.
- [30] D.J. Tantillo, K.N. Houk, *J. Org. Chem.* 64 (1999) 3066, and references therein.
- [31] R.W. Hay, R. Bemby, *Inorg. Chim. Acta* 64 (1982) L179.
- [32] T. Koike, M. Takamura, E. Kimura, *J. Am. Chem. Soc.* 116 (1994) 8443.
- [33] T. Koike, M.S. Kajitani, I. Nakamura, E. Kimura, M. Shiro, *J. Am. Chem. Soc.* 117 (1995) 1210.
- [34] E. Kimura, I. Nakamura, T. Koike, M. Shionoya, Y. Kodama, T. Ikeda, M. Shiro, *J. Am. Chem. Soc.* 116 (1994) 4764.
- [35] C. Bazzicalupi, A. Bencini, A. Bianchi, V. Fusi, C. Giorgi, P. Paoletti, B. Valtacoli, D. Zanchi, *Inorg. Chem.* 36 (1997) 2784.
- [36] R.C. diTargiani, S. Chang, M.H. Salter Jr., R.D. Hancock, D.P. Goldenberg, *Inorg. Chem.* 42 (2003) 5825.
- [37] A. Nomura, Y. Sugiura, *Inorg. Chim. Acta* 43 (2004) 1708.
- [38] A. Bencini, E. Berni, A. Bianchi, V. Fedi, C. Giorgi, P. Paoletti, B. Valtancoli, *Inorg. Chim. Acta* 38 (1999) 6323.
- [39] T.G. Spriggs, C.D. Hall, *J. Chem. Soc. Perkin Trans. 2* (2001) 2063.
- [40] C. Bazzicalupi, A. Bencini, E. Berni, C. Giorgi, S. Maoggi, B. Valtancoli, *Dalton Trans.* (2003) 3574.
- [41] Y. Guo, Q. Ge, H. Lin, H. Lin, S. Zhu, *Int. J. Chem. Kinet.* 36 (2004) 41.
- [42] X. Su, H. Sun, Z. Zhou, H. Lin, L. Chen, S. Zhu, Y. Chen, *Polyhedron* 20 (2001) 91.
- [43] X. Yin, C. Lin, Z. Zhou, W. Chen, S. Zhu, H. Lin, X. Su, Y. Chen, *Transition Met. Chem.* 24 (1999) 537.
- [44] G.E. Means, M.L. Bender, *Biochemistry* 14 (1975) 4989.
- [45] S.S. Massoud, H. Sigel, *Inorg. Chim. Acta* 27 (1988) 1447.
- [46] M.H. Abraham, *Chem. Soc. Rev.* 22 (1993) 73.
- [47] R.W. Hay, N. Govan, *Polyhedron* 15 (1996) 2381.
- [48] R.W. Hay, N. Govan, *Polyhedron* 17 (1998) 463.
- [49] M.M. Ibrahim, K. Ichikawa, M. Shiro, *Inorg. Chim. Acta* 353 (2003) 187.
- [50] R.W. Hay, N. Govan, *Transition Met. Chem.* 23 (1998) 721.
- [51] E. Kimura, Y. Kodama, T. Koike, M. Shiro, *J. Am. Chem. Soc.* 117 (1995) 8304.

- [52] P.E. Jurek, A.E. Martell, *Inorg. Chim. Acta* 287 (1999) 47.
- [53] S.J. Oh, K.H. Song, D. Whang, K. Kim, T.H. Yoon, H. Moon, J.W. Park, *Inorg. Chem.* 35 (1996) 3780.
- [54] K. Yamaguchi, F. Akagi, S. Fujinami, M. Suzuki, M. Shionoya, S. Suzuki, *Chem. Commun.* (2001) 375.
- [55] J. Gao, A. Martell, J. Reibenspies, *Inorg. Chim. Acta* 329 (2002) 122.
- [56] L. Bonfá, M. Gatos, F. Mancin, P. Tecilla, U. Tonellato, *Inorg. Chem.* 42 (2003) 3943.
- [57] M. Area, A. Bencini, E. Berni, C. Caltagirone, F.A. Devillanova, F. Isaia, A. Garau, C. Giorgi, V. Lippolis, A. Perra, L. Tei, B. Valtancoli, *Inorg. Chem.* 42 (2003) 6929.
- [58] L. Zhu, O. dos Santos, C.W. Koo, M. Rybstein, L. Pape, J.W. Canary, *Inorg. Chem.* 42 (2003) 7912.
- [59] C. Vichard, T.A. Kaden, *Inorg. Chim. Acta* 337 (2002) 173.
- [60] M.J. Young, D. Wahnnon, R.C. Hynes, J. Chin, *J. Am. Chem. Soc.* 117 (1995) 9441.
- [61] M. Wall, B. Linkletter, D. Williams, A. Lebuis, R.C. Hynes, J. Chin, *J. Am. Chem. Soc.* 121 (1999) 4710.
- [62] L.M. Rossi, A. Neves, R. Hörner, H. Terenzi, B. Szpoganicz, J. Sugai, *Inorg. Chim. Acta* 337 (2002) 366.
- [63] C. Duboc-Toia, S. Ménage, J.-M. Vincent, M.T. Averbuch-Pouchot, M. Fontecave, *Inorg. Chem.* 36 (1997) 6148.
- [64] A.E. Martel, R.M. Smith, *Critical Stability Constants*, vol. 3, Plenum Press, New York, 1977.
- [65] O. Iranzo, A.Y. Kovalevsky, J.R. Morrow, J.P. Richard, *J. Am. Chem. Soc.* 125 (2003) 1988.
- [66] O. Iranzo, J.P. Richard, J.R. Morrow, *Inorg. Chem.* 43 (2004) 1743.
- [67] L.A. Jenkins, J.K. Bashkin, J.D. Pennock, J. Florián, A. Warshel, *Inorg. Chem.* 38 (1999) 3215.